Published in final edited form as:
J Photochem Photobiol B. 2013 January 5; 118: 33–41. doi:10.1016/j.jphotobiol.2012.10.010.

Contrasting Binding of Fisetin and daidzein in γ-Cyclodextrin Nanocavity

Biswapathik Pahari[1], **Bidisha Sengupta**[2,*], **Sandipan Chakraborty**[3], **Briannica Thomas**[2], **Dyffreyon McGowan**[2], and **Pradeep K. Sengupta**[1,*]

[1]Biophysics Division, Saha Institute of Nuclear Physics, Kolkata, India

[2]Department of Chemistry, Tougaloo College, MS, USA

[3]Saroj Mohan Institute of Technology, West Bengal, India

Abstract

Steady state and time resolved fluorescence along with anisotropy and induced circular dichroism (ICD) spectroscopy provide useful tools to observe and understand the behavior of the therapeutically important plant flavonoids fisetin and daidzein in γ-cyclodextrin (γ-CDx) nanocavity. Benesi-Hildebrand plots indicated 1:1 stoichiometry for both the supramolecular complexes. However the mode of the binding of fisetin significantly differs from daidzein in γ-CDx, as is observed from ICD spectra which is further confirmed by docking studies. The interaction with γ-CDx proceeds mainly by the phenyl rings and partly by the chromone ring of fisetin whereas only the phenyl rings takes part for daidzein. A linear increase in the aqueous solubility of the flavonoids is assessed from the increase in the binding of flavonoids with γ-CDx cavity, which are determined by gradual increase in the ICD signal, fluorescence emission as well as increase in fluorescence anisotropy with increasing [γ-CDx]. This confirms the γ-CDx as a nanovehicle for flavonoids fisetin and daidzein in improving their bioavailability.

Keywords

Excited-state intramolecular proton transfer; Steady state and Time resolved fluorescence spectroscopy; Fluorescence Anisotropy; Induced circular dichroism; Molecular docking

Introduction

Various bioactive flavonoids [1,2] have come into prominence as alternative therapeutic drugs in the past few decades, due to their important therapeutic activities with high potency and low systemic toxicity, which is marked by an explosive growth of research in this area

*Corresponding authors: Pradeep K. Sengupta, Biophysics Division, Saha Institute of Nulcear Physics, Kolkata 700064, India. pradeepsinp@yahoo.co.in; pradeepk.sengupta@saha.ac.in (phone:+919831393962). Bidisha Sengupta, Department of Chemistry, Tougaloo College, Tougaloo, MS 39174, U.S.A. bsengupta@tougaloo.edu; bsgupta.tougaloo@gmail.com (phone: +1-601-977-7779, FAX: +1-601-977-7898).

Supporting Information Available: Figures 1S and 2S are displayed in the supporting information. The polarity of the γ-CDx cavity is studied using solvents of different dielectric constants as references, which is displayed in Figure 1S. The typical fluorescence emission of daidzain in free and γ-CDx bound states along with absorption and excitation spectra are shown in Figure 2S. This material is available free of charge via the Internet at http://pubs.acs.org.

[1–10]. Many recent studies, both in vivo and in vitro, have established that flavonoids are powerful antioxidants effective against a wide range of free radical mediated and other diseases including various types of cancers, tumors, diabetes mellitus, atherosclerosis, ischemia, neuronal degeneration, cardiovascular ailments, and AIDS [3–8]. The flavonol fisetin (3,3′,4′,7-tetrahydroxyflavone, Scheme 1) is a flavonoid present in a number of commonly eaten foods, such as strawberries, vegetables, nuts and wine [9], and has been reported to protect nerve cells from oxidative stress-induced death [10] and promote the differentiation of nerve cells [11]. Fisetin is also found to inhibit Aβ fibril formation in vitro [12,13]. In vivo, fisetin has recently been shown to possess interesting anticancer activity in lung carcinoma [14], prostate tumours [15], and human embryonal carcinoma [16] in mice. Another flavonoid of contemporary interest is the isoflavone daidzein (7-hydroxy-3(-4′-hydroxy-phenyl)-chromen-4-one, Scheme 1), commonly found in legumes.[17] daidzein has a wide spectrum of physiological and pharmacological functions including antiestrogenic [18, 19], anticancer [20, 21], anti-inflammatory [22], cardioprotective [23] and enzyme-inhibitory effects [18, 19]. Another important and interesting feature of fisetin and other structurally related flavonoids, is their dual fluorescence behavior [7,24–26], which shows remarkable sensitivity to the surrounding microenvironment serving as exquisitely sensitive fluorescent molecular probes. Despite the vast importance of the bioflavonoids as therapeutic drugs for the treatment of cancer and other diseases, their administration in vivo remains problematic partly due to their poor water solubility [27–30]. Encapsulation of the drugs into polymer-based nanoparticles appears to markedly help the oral delivery of flavonoids in three ways: 1. By increasing solubility, 2. by protecting the drug from degradation in the gastrointestinal tract, and 3. by virtue of their unique absorption mechanism through the lymphatic system and first-pass metabolism in the liver [30]. Hence, to improve the solubility of fisetin and daidzein, thereby improving their *in vivo* administration, we chose γ-cyclodextrin [28, 30] as a suitable molecular carrier to achieve a better bioavailability.

Cyclodextrins are capable of enhancing the solubility, dissolution rate and membrane permeability [28,29] of such drugs. Cyclodextrins (CDxs) are cyclic oligosachharides which consist of (1,4)-linked α-D-glucopyranose units and are produced by enzymatic degradation of starch by cyclodextrin glycosyltransferase (CGTase) [31,32]. The properties of the natural cyclodextrins (CDxs), their complexes and derivatives seem to be surprising because the 7-membered β-CDx (with cavity diameter 0.6–0.66 nm) is the least soluble (at 25 °C solubility in water is 18.5 mg/cm^3), the 6-membered α-CDx (0.47–0.53 nm) is more soluble (solubility in water is 130 mg/cm^3), and the 8-membered γ-CDx (0.75–0.83) (Scheme 2) attains the highest solubility (solubility in water is 300 mg/cm^3) [31, 32]. The aim of the present study is therefore to characterize γ–CDx as the nano vehicle of fisetin and daidzein that could be suitable for parenteral administration.

Materials and methods

Experimental

Fisetin, daidzein and γ-cyclodextrin are purchased from Sigma-Aldrich Chemical Company and used as obtained. The solvents used are of spectroscopic grade and checked for any absorbing and/ or fluorescent impurities. The final concentration of fisetin and daidzein are kept in the order of 10^{-6} M and methanol/ethanol concentrations are below 1% v/v. Stock γ-CDx solutions are prepared by dissolving requisite amount of cyclodextrin powder in deionized water. To prepare each solution for spectroscopic measurements requisite amounts of flavonoids from concentrated ethanolic stock solution are added in cyclodextrin solutions and mixed with gentle shaking for a few minutes.

Spectroscopic Measurements

Steady state absorption spectra are recorded with Shimadzu UV2550 spectrophotometer with Peltier temperature controller. Steady state fluorescence measurements are carried out with Shimadzu RF5301 and Varian Cary-Eclipse spectrofluorometers. Steady state fluorescence anisotropy (*r)* values are calculated using the expression

$$r=\frac{I_{VV}-GI_{VH}}{I_{VV}+2GI_{VH}};$$

where I_{VV} and I_{VH} are the vertically and horizontally polarized components of the flavonoid emission after excitation by vertically polarized light at the respective wavelength. G is the sensitivity factor of the detection systems [33]. Time resolved fluorescence decay measurements are performed using Jobin–Yvon nanosecond time correlated single photon counting (TCSPC) setup. As excitation source a 340 nm nano LED having pulse FWHM ~ 950 ps and a 375 nm laser diode having pulse FWHM ~ 170 ps are used. An emission monochromator is used to block scattered light and isolate the emission. Data analyses are performed using DAS6 Fluorescence Decay Analysis Software, provided with the TCSPC instrument and are fitted with a multi exponential decay function, or $I(t)=\sum_i a_i \exp(t/\tau_i)$ where a_i and τ_i represent the amplitudes and decay times respectively of the individual components for multi-exponential decay profiles. The goodness of fit is estimated by using reduced χ^2 (namely χ^2_R) values as well as Durbin–Watson parameters (DW). A fit is considered acceptable for a given set of observed data and chosen function, when the χ^2_R value is in the range 0.8–1.2 and the DW value is greater than 1.7, 1.75 and 1.8 for a single, double and triple exponential fit respectively [33]. Average lifetime is calculated using the equation, $\bar{\tau}=\frac{\sum_i a_i \tau_i^2}{\sum_i a_i \tau_i}$ where a_i and τ_i represent the amplitude and decay time respectively of the individual components for multi-exponential decay profiles. Circular dichroism spectra are acquired with Biologic Science Instruments (France) spectropolarimeter, using a rectangular cuvette with 1 cm path length. The scan rate is 60–100 nm/min, and three/five consecutive spectra are averaged to produce the final spectrum. All spectral measurements are performed at ambient temperature. The highest concentration of γ-CDx for fluorescence decay, anisotropy (steady state), and circular dichroism experiments are kept at ~20 mM in order to avoid scattering and artifacts.

Theoretical study

Docking study—To identify the possible modes of fisetin and daidzein binding with γ-cyclodextrin, docking studies have been performed with Lamarkian genetic algorithm implemented in AutoDock (version 4.0) [34,35]. The initial structures of fisetin and daidzein are built using HYPERCHEM 7.5 [36] molecular builder and optimized using PM3 method to RMS convergence of 0.01 kcal/Å.mol with Polak-Ribiere conjugate gradient algorithm. The γ-CDx structure is obtained from the crystal structure of a γ-CDx complex available in Protein Data Bank (PDB ID-2ZYK). γ-CDx structure is also optimized by semi empirical method (PM3) to RMS convergence of 0.01 kcal/Å.mol with Polak-Ribiere conjugate gradient algorithm and used as a starting structure in the docking study. Non-polar hydrogens are merged and partial atomic charges are calculated using Gasteiger-Marsili method. Rotatable bonds are also assigned for both fisetin and daidzein. The grid maps are

calculated using AutoGrid. The grid box is set to 40 × 40 × 40 point cubic box with a grid spacing 0.375 A centered on γ-CDx. The grid box is chosen to be significantly large to include not only the cavity portion but also to cover the entire cyclodextrin surface. 250 docking runs are carried out and for each run, a maximum of 2,500,000 GA operations are performed on a single population of 150 individuals. The weights for crossover, mutation and elitism are default parameters (0.8, 0.02 and 1 respectively). Parameters used for the docking herein, have been successfully applied in previous studies on the inclusion of other flavonoids and hydrophobic molecules of related interests within cyclodextrin cavity [37–39].

Results and observations

Steady State Fluorescence Spectroscopy

Figures 1A and B present the fluorescence emission and excitation spectra and figure 1C presents the absorption spectra of fisetin with increasing concentration of γ-cyclodextrin. It is evident that addition of γ-cyclodextrin induces dramatic changes in the emission behavior of fisetin. In aqueous medium, the fluorescence spectra of fisetin exhibits strong overlap between the normal and tautomer emission bands [24]. With the addition of the γ-cyclodextrin, dual fluorescence behavior is observed. The emission spectra of fisetin consist of two color' fluorescence bands, namely a yellow-green emission band along with a high energy band in the blue-violet region. The blue-violet fluorescence is assigned to the S_1 ($\pi\pi^*$)→S_0 normal (non-proton transferred) emission, the large Stokes shifted green fluorescence is attributed to emission from a tautomer species generated by an excited state intramolecular proton transfer (ESPT) process occurring along the internal H-bond (C(4)=O---HO–C(3)) of the molecule (Scheme 1) [24]. The "blue-violet" and "yellow-green" fluorescence emissions occur from N* and T* species respectively (Scheme 1). The intensity ratio of tautomer : normal fluorescence (I_T / I_N) increases rapidly with increasing CDx concentration (shown in Fig. 1A inset), until [CDx] ~20 mM beyond which it tends to level off. These observations can be rationalized in terms of interference with the internal H-bond of fisetin which permits the ESPT process. It is noteworthy that the emission profiles of fisetin recorded in the cyclodextrin environment resemble the situation in aprotic environment where dual emission behavior is prominent [40] (Figures 1A and 1S). Moreover, this is consistent with the spectral characteristics of the excitation profile (monitored for the PT fluorescence) which reveals a weak but clearly perceptible vibrational shoulder (Figure 1B) [40] typical of a predominantly aprotic environment. The absorption spectrum of fisetin after binding with γ-CDx does not show any change in peak position indicating that no additional species of fisetin is generated. The enhanced tautomer emission as well as the strongly red shifted (~22 nm for tautomer from 0 to 50 mM γ-CDx) fluorescence band, indicate that the guest (fisetin) molecules experience relatively aprotic environments, in the CDx microenvironment (see Table 1, Figure 1). The emission behavior of fisetin inside the γ-CDx cavity closely resemble that in EtOH-water mixture and aprotic solvent systems [41] at lower and higher concentrations of γ-CDx respectively (Figures 1 and 1S), which agrees well with the literature data [32,42].

Figure 2S and Table 1 reveals the behavior of 10 μM daidzein in γ-CDx. Interestingly, unlike fisetin, daidzein being an isoflavone, does not have an HO–C(3) (see Scheme 1) hydroxyl group, which precludes any internal hydrogen bond and ESPT. Upon incorporation in CDx, the fluorescence intensity of daidzein increases with increasing [γ-CDx] as is shown in Figure 2SA and inset. However the excitation (Figure 2S B) and absorption spectra (Figure 2S C) indicate the absence of any newly generated species of daidzein in CDx upon forming the supramolecular complex.

Steady state fluorescence anisotropy

Fluorescence anisotropy (r) serves as a sensitive indicator for monitoring fluorophore binding to motionally constrained regions of matrix [33]. Steady state fluorescence anisotropy for both fisetin (for ESPT tautomer species, Scheme 1) and daidzein (see Table 1) show dramatic enhancements on gradual addition of γ-CDx [Figure 2, solid and dashed lines indicating fisetin and daidzein respectively], suggesting that the fisein and daidzein molecules are confined in the motionally constrained nanocavities of CDx where rotational diffusions are reduced. Progressive increase in the anisotropy (in free solution r' is very low) [28] of the fluorophore emission is observed which is consistent with the picture that more and more flavonoid molecules are occurring in γ-CDx bound states. This restriction of motion of the flavonoids in CDx nanocavity induces an increase in the solubility of the flavonoids (fisetin and daidzein) in aqueous environment because CDx is prepared in aqueous solution. Hence it can be inferred that restricted motions of flavonoids (as is evident from increased fluorescence anisotropy) in γ-CDx matrix, indirectly helps the dissolution of flavonoids in aqueous system, thereby making them more bioavailable. Although the overall anisotropy of daidzein and fisetin do not differ significantly in 20 mM γ-CDx, but the mode of increase of r' with gradual increase in [CDx] differs, suggesting that the binding modes of flavonol fisetin and isoflavone daidzein are different.

Fluorescence decay analysis by TCSPC studies

Time-resolved fluorescence decay studies provide useful information for the understanding of the photophysical processes of a fluorescent probe in the excited state. These are performed to examine how confinement in the γ-CDx cavities influences the fluorescence decay profiles of the flavonoids when compared to the free state in aqueous systems. The normal species along with the ESPT tautomer emission decay kinetics of fisetin and daidzein (normal species only) are studied in aqueous and γ-CDx systems. The results are presented in Table 2, Figure 3 for fisetin and Table 3, Figure 4 for daidzein. The fluorescence intensity decay of fisetin ESPT tautomer species in absence of γ-CDx can be fitted by a double exponential function with an average decay ($\bar{\tau}$) of 0.7 ns which is in agreement with a recent report [4]. Upon inclusion into γ-CDx, there is a dramatic change in the decay kinetics of fisetin tautomer species. In γ-CDx, three discrete decay components are observed, which can be attributed to the different extent of inter molecular H-bond of fisetin with the matrix. $\bar{\tau}$ increases by five times in 10 mM γ-CDx (4.99 ns) and 20 mM γ-CDx (5.55 ns) environments. Furthermore, $\bar{\tau}$ increases (~ 11%) with increase in γ-CDx concentration from 10 mM to 20 mM (Table 2), with significant increase in decay time of all decay components. However the changes in $\bar{\tau}$ and population distribution of the normal species of fisetin in γ-CDx are less significant in γ-CDx matrix as is shown in Figure 3 and Table 2. The nonexponential decay in presence of high concentration of γ-CDx indicates heterogeneity in the micro-environments of fisetin in the γ-CDx nanocavity. It is pertinent to mention that the microenvironment near the edge of the cyclodextrin cavity resembles the properties of a binary aqueous solvent (e.g. EtOH : water) [32] while the interior of the γ-CDx cavity is similar in polarity to oxygenated solvents such as dioxane, isopropyl ether, and ethylene glycol [42] which agrees well with Figure 1S. The multiple decay components observed for the tautomer species of fisetin is likely to arise from populations differing in the extent of H-bonding within the microenvironment of γ-CDx. Furthermore, we note that for the ESPT tautomer species of fisetin, the individual decay component of the cyclodextrin encapsulated fisetin molecules have significantly higher decay time compared to those observed in water (Table 2) indicating that the fisetin molecules experience relatively hydrophobic microenvironments within the γ-CDx cavities where non-radiative decay processes are reduced [43]. This is also reflected in the spectacular increase in emission yield upon addition of the γ-CDx (see Figure 1 and inset).

In case of daidzein dissolved in water the decay profile can be fitted to a mono-exponential decay function with decay time 1.32 ns. This readily changes to a bi-exponential decay function with a significant increase in $\bar{\tau}$ (~60% from water to 20 mM γ-CDx) upon addition of γ-CDx indicating the emission arises from populations differing in the extent of H-bonding with the microenvironment that we have discussed before. $\bar{\tau}$ increases ($\bar{\tau}$~ 1.3 ns in water, and ~ 2 ns in γ-CDx) upon inclusion in γ-CDx matrix. Population of faster decay component decreases ($\bar{\tau}$~ 1.3 ns, 100% in water, 68% in 10 mM and 41% in 20 mM γ-CDx) from water with increasing [CDx] whereas the reverse is observed for the slower component (~ 2.5 ns, nil in water, 32% in 10 mM and 59% in 20 mM γ-CDx). The faster component arises from daidzein in aqueous medium whereas the slower decay component appears from daidzein encapsulated inside aprotic γ-CDx nano-cavity where solvent molecules mediated perturbations and non-radiative transitions are largely diminished, giving rise to higher emission and slow decay time (Figures 2S and 4, Table 3). It is pertinent to mention here that the extent of increase of fluorescence lifetime is not same for both the flavonoids because their inherent fluoresecence properties are different [7,17].

Induced circular dichroism (ICD) spectroscopic study

To further characterize the fisetin-γ-CDx and daidzein-γ-CDx inclusion complexes, circular dichroism (CD) spectroscopic studies have been performed. When an intrinsically optically inactive molecule binds to a chiral host, the asymmetric environment of the host induces optical activity in the guest molecule. This results in appearance of induced circular dichroism (ICD) bands in the absorption region of the guest [44]. Occurrence of ICD bands therefore provides a sensitive spectroscopic characterization of such host–guest interactions. Fisetin and daidzein being achiral in nature do not show any CD bands in solvent media (e.g. water or aqueous methanol). Interestingly on addition of γ-CDx, pronounced ICD bands appear in the far and near UV region (Figures 5 A and B) indicating complex formation of the fisetin and daidzein with γ-CDx molecules. The observation of ICD signals in this region, corresponding to the electronic transitions, indicates that the fisetin and daidzein molecules experience strong interactions with the chiral skeleton of the γ-CDx nanocavity. The increase in ICD signal for fisetin at 390 nm is more profound than daidzein at 340 nm, which support the interpretation from fluorescence anisotropy regarding their difference in mode of binding in γ-CDx nanocavity. The strong and most significant ICD signals at ~ 250 and ~ 390 nm, are attributed to the A–C and B–C rings respectively for daidezein and fisetin [45]. It is pertinent to mention that these wavelengths mostly correspond to their respective absorption and fluorescence excitation spectra (Figures 1 and 2S). Rings A, B, C take part in binding fisetin with CDx. It is likely that binding occurs primarily through the phenyl ring B with two–OH and ring A with one –OH groups and partly through the chromone ring C (because it takes part in forming the ESPT species, see Scheme 1). On the other hand, despite the free –C=O in ring C of daidzein (no ESPT), the steric congestion arising from the ring B at the C-3 position of daidezein, makes the single –OH groups of phenyl ring B and A to interact with CDx cavity.

Measurements of binding parameters

Since the value of the binding constant gives an idea about the strength of the binding interaction and highlights the mode of binding, we have exploited the circular dichroism titration data and the modified Benesi-Hildebrand equation [46] as follows to determine the binding constant (Figure 6) between fisetin and γ-CDx.

$$\frac{1}{\Delta\theta}=\frac{1}{\Delta\theta_{\max}}+\frac{1}{\Delta\theta_{\max}K_a[\gamma\text{-}CD]} \quad (2)$$

Here $\Delta\theta = \theta_x - \theta_0$ and θ_x, θ_0 represent the ellipticity of fisetin at 390 nm and daidzein at 250 nm in the presence and absence of total added γ-CDx concentrations, respectively. $\Delta\theta_{max}$ is the maximum change in the ellipticity at 390 nm and 250 nm for fisetin and daidzein respectively and K_a is the association constant for the 1:1 complex. A plot of $1/\Delta\theta$ against $[\gamma\text{-}CDx]^{-1}$ gives a straight line justifying the validity of the above equation and hence confirming one-to-one interaction between the flavonoids and the cyclodextrin. The association constants for the fisetin-γ-CDx and daidzein-γ-CDx complexes are found to be 1.46 (± 0.36) x 10^3 M^{-1} and 3.81(± 0.71) x 10^2 M^{-1}, which are obtained from the slope of the best fit straight lines in the plots, where cyclodextrin concentration is taken on molar scale [Figure 6 A, B]. The higher K_a value of fisetin compared to daidzein justifies the interpretation from ICD results.

Molecular docking studies

In order to rationalize our experimental data and infer about the mode of inclusion, we performed molecular docking studies of fisetin and daidzein with γ-CDx by using AutoDock. The lowest energy docked complex of fisetin and daidzein within γ-CDx nano-cavity reveals a contrasting mode of inclusion for the two flavonoids, shown in Fig. 7.

For the fisetin-γ-CDx inclusion complex, it is observed that the B-ring of fisetin is deeply embedded into the cavity and face toward the primary hydroxyl group of the CDx cavity (Figure 7). Consistent with the fluorescence results, the docking study also shows that the chromone moiety of fisetin is readily incorporated into the relatively less polar cavity of γ-CDx and facing the secondary hydroxyl rim of the γ-CDx cavity. Interestingly, the intra-molecular hydrogen bonding, between C(3)-OH and C(4)=O group, of fisetin that is responsible for the ESPT process is preserved within the γ-CDx cavity. This mode of inclusion is further supported by the fact that CD spectroscopy reveals an induced CD (ICD) band ~ 390 nm (see Figure 5) which corresponds to the absorption band I of flavonoids attributed to the absorption from the B+C ring of flavonoids. In contrast to fisetin, daidzein inclusion occurs mainly through A+C ring of the flavonoid and the B-ring is exposed to the secondary hydroxyl rim of the γ-CDx cavity. Interestingly, ICD spectra reveal ICD bands ~ 250 nm (see Figure 5) corresponding to the absorption band II which is attributed to the absorption from the A+C ring of flavonoids [45]. Furthermore, the larger volume of the γ-CDx cavity allows tilted orientation of the flavonoid molecular axis with respect to the symmetry axis of the CDx cavity, which maximizes the hydrogen bonding possibilities. The hydrogen bonding interactions are found to be important energetic factors that facilitate formation of the inclusion complex along with van der Waals interactions. Fisetin forms three hydrogen bonds with γ-CDx cavity. In particular, 3′-OH and 4′-OH groups of the B-ring of fisetin (as H-bond donor) are involved in hydrogen bonding interactions with the OH groups of the primary hydroxyl rim of γ-CDx while the 7-OH group (as H-bond donor) forms hydrogen bond with the wider secondary hydroxyl rim of γ-CDx cavity. On the other hand daidzein is involved in two hydrogen bonding interactions with γ-CDx: the 7-OH group (as H-bond donor) forms hydrogen bond with the primary hydroxyl rim while the 4′-OH group (as H-bond donor) is involved in hydrogen bonding interaction with the secondary hydroxyl OH group of the γ-CDx. The γ-CDx cavity acts as the H-bond acceptor for both the flavonoids. These differences in the number of possible hydrogen bonds account for the observed higher binding affinity of fisetin with γ-CDx compared to daidzein.

Summary and Concluding Remarks

Complexation of molecules to cyclodextrin occurs through a non-covalent interaction between the molecule and the CDx cavity. Dramatic changes are evident from the steady state and time resolved fluorescence as well as circular dichroism spectroscopic studies of fisetin and daidzein in CDx microenvironment when compared to that in water. However the

mode of binding varies remarkably for these two different kinds of flavonoids as is depicted through ICD, fluorescence anisotropy and docking studies. This binding is a dynamic process whereby the guest molecule continuously associates and dissociates from the host CDx. Establishing a biocompatible nanovehicle for increasing bioavailability of therapeutically important two different kinds of therapeutically important dietary flavonoids, mainly the flavonol fisetin and the isoflavone daidzein, was the key factor for undertaking this study. Commercially CDs are well accepted because of their low systemic (oral, eye, mucous) toxicity and easy availability, which confirms the importance of this investigation on their binding modes through spectroscopic and docking studies. From our present findings, γ-CDx appears to be an important carrier where structural variations in the guest flavonoids result in different binding modes and affinities for the host cavity.

Supplementary Material

Refer to Web version on PubMed Central for supplementary material.

Acknowledgments

BSG likes to thank the financial support from NIH/ NCMHHD/RIMI grant # 1P20MD002725 and research support from HBCU-UP Grant, NSF ID: 0811638 and Epscor grant MS- EPS-0903787, at Tougaloo College. PKS gratefully acknowledges CSIR, India for the award of a grant under CSIR Emeritus scientist scheme, sanction no. 21(0864)/11/EMR-II. We thank Professor Abhijit Chakrabarti of Structural Genomics Division of SINP for letting us use the circular dichroism spectrometer and Mr. Subrata Das of the Department of Spectroscopy, IACS, Kolkata for assistance with picosecond time resolved data collection and analysis.

References

1. Rusznyák, St; Szent-Györgyi, A. Nature. 1936; 138:27–27.
2. Mabry, TJ.; Markham, KR.; Thomas, MB. The Systematic Identification of Flavonoids. Springer-Verlag; Heidelberg, New York, Berlin: 1970.
3. Lagiou P, Samoli E, Lagiou A. Intake of specific flavonoid classes and coronary heart disease a case-control study in Greece. Eur J Clin Nutr. 2004; 58:1643–1648. [PubMed: 15226759]
4. Selvam T, Mishra AK. Multiple prototropism of fisetin in sodium cholate and related bile salt media. Photochem Photobiol Sci. 2011; 10:66–75. [PubMed: 20976368]
5. Havsteen BH. The biochemistry and medical significance of the flavonoids. Pharmacol Ther. 2002; 96:67–202. [PubMed: 12453566]
6. Middleton E Jr, Kandaswami C, Theoharides TC. The effects of plant flavonoids on mammalian cells: implications for inflammation, heart disease, and cancer. Pharmacol Rev. 2000; 52:673–751. [PubMed: 11121513]
7. Sengupta B, Banerjee A, Sengupta PK. Investigations on the binding and antioxidant properties of the plant flavonoid fisetin in model biomembranes. FEBS Letters. 2004; 570:77–81. [PubMed: 15251443]
8. Mohapatra M, Mishra AK. Photophysical Behavior of Fisetin in Dimyristoylphosphatidylcholine Liposome Membrane. J Phys Chem B. 2011; 115:9962–9970. [PubMed: 21766844]
9. Arai Y, Watanabe S, Kimira M, Shimoi K, Mochizuki R, Kinae N. Dietary intakes of flavonols, flavones and isoflavones by Japanese women and the inverse correlation between quercetin intake and plasma LDL cholesterol concentration. J Nutr. 2000; 130:2243–2250. [PubMed: 10958819]
10. Ishige K, Schubert D, Sagara Y. Flavonoids protect neuronal cells from oxidative stress by three distinct mechanisms. Free Radical Biol Med. 2001; 30:433–446. [PubMed: 11182299]
11. Sagara Y, Vanhnasy J, Maher P. Induction of PC12 cell differentiation by flavonoids is dependent upon extracellular signal-regulated kinase activation. J Neurochem. 2004; 90:1144–1155. [PubMed: 15312169]
12. Akaishi T, Morimoto T, Shibao M, Watanabe S, Sakai-Kato K, Utsunomiya-Tate N, Abe K. Structural requirements for the flavonoid fisetin in inhibiting fibril formation of amyloid beta protein. Neurosci Lett. 2008; 444:280–285. [PubMed: 18761054]

13. Ushikubo H, Watanabe S, Tanimoto Y, Abe K, Hiza A, Ogawa T, Asakawa T, Kan T, Akaishi T. 3,3′,4′,5,5′-Pentahydroxyflavone is a potent inhibitor of amyloid β fibril formation. Neurosci Lett. 2012; 513:51–56. [PubMed: 22343025]
14. Touil YS, Seguin J, Scherman D, Chabot GG. Improved antiangiogenic and antitumour activity of the combination of the natural flavonoid fisetin and cyclophosphamide in Lewis lung carcinoma-bearing mice. Cancer Chemother Pharmacol. 2011; 68:445–455. [PubMed: 21069336]
15. Khan N, Asim M, Afaq F, Abu ZM, Mukhtar H. A novel dietary flavonoid fisetin inhibits androgen receptor signaling and tumor growth in athymic nude mice. Cancer Res. 2008; 68:8555–8563. [PubMed: 18922931]
16. Tripathi R, Samadder T, Gupta S, Surolia A, Shaha C. Anticancer activity of a combination of cisplatin and fisetin in embryonal carcinoma cells and xenograft tumors. Mol Cancer Ther. 2011; 10:255–268. [PubMed: 21216935]
17. Sengupta B, Chakraborty S, Crawford M, Taylor JM, Blackmon LE, Biswas PK, Kramer WH. Characterization of daidzein–hemoglobin binding using optical spectroscopy and molecular dynamics simulations. Int J Biol Macromol. 2012; 51:250–258. [PubMed: 22609682]
18. Setchell KDR, Cassidy A. Dietary isoflavones: biological effects and relevance to human health. J Nutr. 1999; 129:758–767.
19. Jacobsen BK, Knutsen SF, Fraser GE. Does high soy milk intake reduce prostate cancer incidence? The Adventist Health Study (United States). Cancer Causes Control. 1998; 9:553–557. [PubMed: 10189040]
20. Esselen M, Boettler U, Teller N, Bachler S, Hutter M, Rufer CE, Skrbek S. 7D. Marko, Anthocyanin-rich blackberry extract suppresses the DNA-damaging properties of topoisomerase I and II poisons in colon carcinoma cells. J Agric Food Chem. 2011; 59:6966–73. [PubMed: 21599019]
21. Setchell KDR, Brown NM, Desai PB, Zimmer-Nechimias L, Wolfe B, Jakate AS, Creutzinger V, Heubi JE. Bioavailability, Disposition, and Dose-Response effects of Soy Isoflavones when consumed by healthy women at physiologically typical dietary intakes. J Nutr. 2003; 133:1027–1035. [PubMed: 12672914]
22. Prochazkova D, Bousova I, Wilhelmova N. Antooxidant and prooxidant properties of flavonoids. Fitoterapia. 2011; 82:513–523. [PubMed: 21277359]
23. Manach C, Mazur A, Scalbert A. Polyphenols and prevention of cardiovascular diseases. Curr Opin Lipidol. 2005; 16:77–84. [PubMed: 15650567]
24. Sengupta PK, Kasha M. Excited state proton-transfer spectroscopy of 3- hydroxyflavone and quercetin. Chem Phys Lett. 1979; 68:382–385.
25. Sengupta B, Banerjee A, Sengupta B. Interactions of the plant flavonoid fisetin with macromolecular targets: Insights from fluorescence spectroscopic studies. J Photochem Photobiol B. 2005; 80:79–86. [PubMed: 16038806]
26. Demchenko AP, Ercelen S, Roshal AD, Klymchenko AS. Excited-state proton transfer reaction in a new benzofuryl 3-hydroxychromone derivative: the influence of low polar solvents. Polish J Chem. 2002; 76:1287–1299.
27. Mignet N, Seguin J, Ramos Romano M, Brullé L, Touil YS, Scherman D, Bessodes M, Chabot GG. Development of a liposomal formulation of the natural flavonoid fisetin. Int J Pharm. 2012; 423:69–76. [PubMed: 21571054]
28. Banerjee A, Sengupta PK. Encapsulation of 3-hydroxyflavone and fisetin in b-cyclodextrins: Excited state proton transfer fluorescence and molecular mechanics studies. Chem Phys Lett. 2006; 424:379–386. and references cited therein.
29. Borghetti GS, Pinto AP, Lula IS, Sinisterra RD, Teixeira HF, Bassani VL. Daidzein / cyclodextrin/ hydrophilic polymer ternary systems. Drug Dev Ind Pharm. 2011; 37:886–893. [PubMed: 21247375]
30. Leonarduzzi G, Testa G, Sottero B, Gamba P, Poli G. Design and development of nanovehicle-based delivery systems for preventive or therapeutic supplementation with flavonoids. Curr Med Chem. 2010; 17:74–95. [PubMed: 19941477]
31. Shimpi S, Chauhan B, Shimpi P. Cyclodextrins: Application in different routes of drug administration. Acta Pharm. 2005; 55:139–156. [PubMed: 16179128]

32. Szejtli J. Past, present, and future of cyclodextrin research. Pure Appl Chem. 2004; 76:1825–1845. and references cited therein.
33. Lakowicz, JR. Principles of Fluorescence Spectroscopy. Springer; 2006.
34. Morris GM, Goodsell DS, Halliday RS, Huey R, Hart WE, Belew RK, Olson AJ. Automated Docking Using a Lamarckian Genetic Algorithm and and Empirical Binding Free Energy Function. J Computational Chemistry. 1998; 19:1639–1662.
35. Morris GM, Goodsell Huey DSR, Olson AJ. Distributed automated docking of flexible ligands to proteins: Parallel applications of AutoDock 2.4. J Computer-Aided Molecular Design. 1996; 10:293–304.
36. Hyperchem, Hypercube Inc; USA: 2002.
37. Pahari B, Chakraborty S, Sengupta PK. Encapsulation of 3-hydroxyflavone in γ-cyclodextrin nanocavities: Excited state proton transfer fluorescence and molecular docking studies. J Mol Struct. 2011; 1006:483–488.
38. Chakraborty S, Basu S, Lahiri A, Basak S. Inclusion of chrysin in β-cyclodextrin nanocavity and its effect on antioxidant potential of chrysin: A spectroscopic and molecular modeling approach. J Mol Struct. 2010; 977:180–188.
39. Chaudhuri S, Chakraborty S, Sengupta PK. Encapsulation of serotonin in b-cyclodextrin nano-cavities: Fluorescence spectroscopic and molecular modeling studies. J Mol Struct. 2010; 975:160–165.
40. Guharay J, Dennison SM, Sengupta PK. Influence of different environments on the excited-state proton transfer and dual fluorescence of fisetin. Spectrochim Acta A. 1999; 55:1091–1099. and references cited therein.
41. Wyman J. The Dielectric constant of mixtures of ethyl alcohol and water from −5 to 40. J Am Chem Soc. 1931; 53:3292–3301.
42. Frankewich RP, Thimmaiah KN, Hinze WL. Evaluation of the Relative Effectiveness of Different Water-Soluble β-Cyclodextrin Media To Function as Fluorescence Enhancement Agents. Anal Chem. 1991; 63:2924–2933.
43. Banerjee A, Basu K, Sengupta PK. Effect of b-cyclodextrin nanocavity confinement on the photophysics of robinetin. J Photochem Photobiol B Biol. 2007; 89:88–97.
44. Allenmark S. Induced circular dichroism by chiral molecular interaction. Chirality. 2003; 15:409–422. [PubMed: 12692886]
45. Anouar EH, Gierschner J, Duroux JL, Trouillas P. UV/Visible spectra of natural polyphenols: A time-dependent density functional theory study. Food Chem. 2012; 131:79–89.
46. Xiang TX, Anderson BD. Inclusion complexes of purine nucleosides with cyclodextrins II. Investigation of inclusion complex geometry and cavity microenvironment. Int J Pharm. 1990; 59:45–55.

Highlights

- Fisetin/γ–cyclodextrin and daidzein/γ–cyclodextrin inclusion complexes were prepared and contrasting binding modes were explored.
- Steady state spectroscopic analyses confirmed the supramolecular interaction of complexes.
- 1:1 stoichiometry of the complexes of flavonoid-γ-CDx was determined from ICD spectra.
- Increased fluorescence anisotropy and lifetime assures increased solubility of the flavonoids.
- Molecular docking reveals hydrogen bonding primarily dictates the inclusion complex formation.

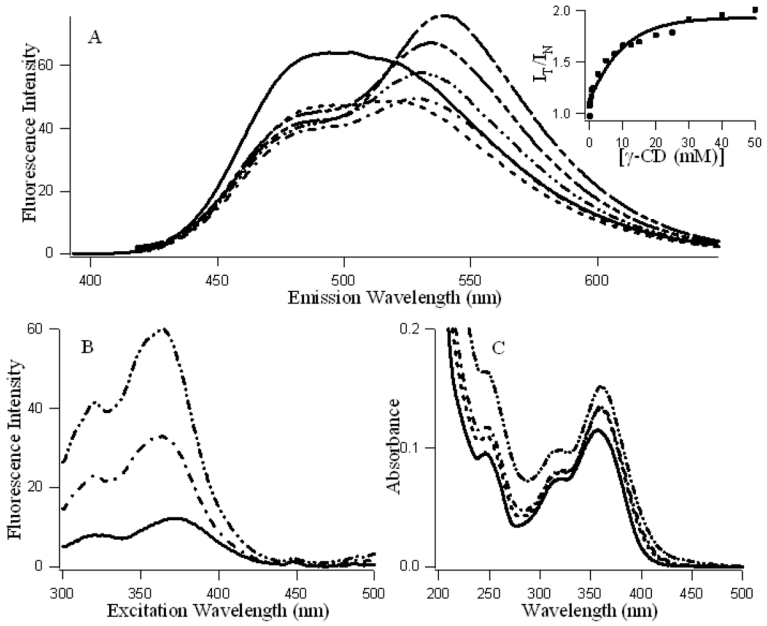

Figure 1.

A: Fluorescence emission spectra (λ_{ex} = 380 nm), B: Fluorescence excitation spectra (λ_{em} = 530 nm) and C: Absorption spectra of fisetin (~ 7.5 μM) in presence of increasing concentrations of γ-cyclodextrin (0—, 1 ---, 5 –·–, 10 –··–, 20 –···–, 50 mM – – --). A_{inset}: Variation of the ratio of the intensity of tautomer vs normal isomers of fisetin ($I_{T\ at\ 530}$ / $I_{N\ at\ 470}$) with increasing [γ-cyclodextrin].

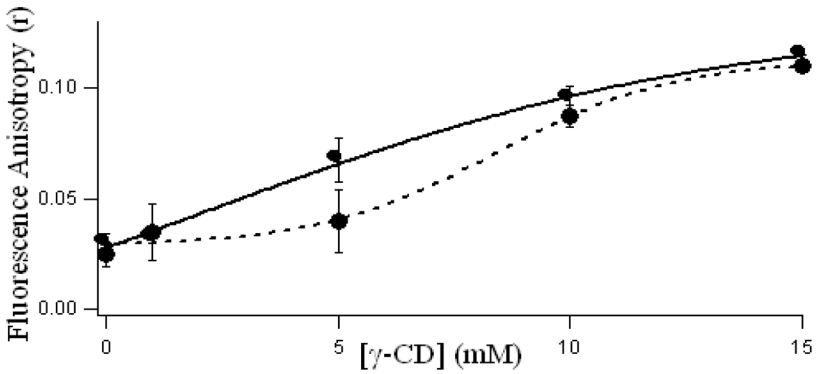

Figure 2.
Variation of steady state fluorescence anisotropy (*r*) of fisetin (7.5 μM) ESPT tautomer species (—, λ_{ex} = 380 nm, λ_{em} = 580nm) and daidzein (10 μM, - - -, λ_{ex} = 340 nm, λ_{em} = 470 nm) with γ-cyclodextrin concentration.

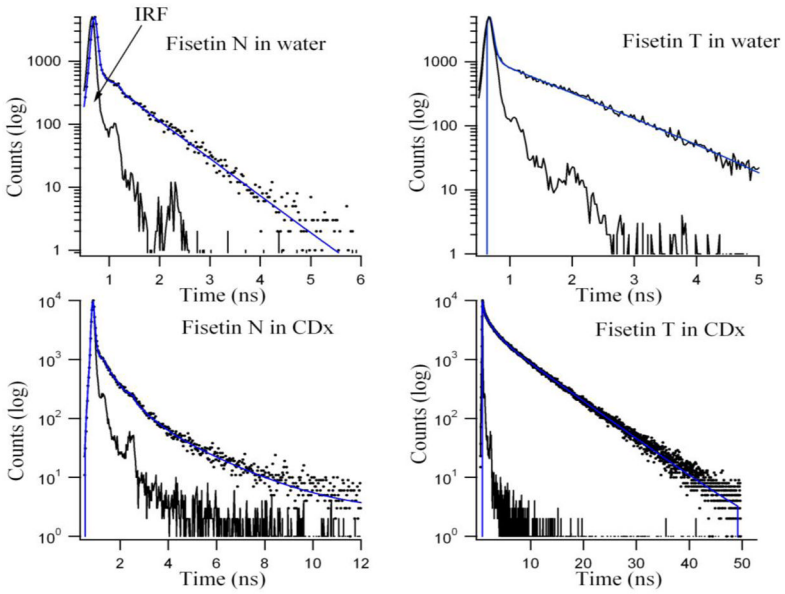

Figure 3.

Fluorescence decay profiles for 7.5 μM fisetin normal (N) and ESPT tautomer (T) in 20 mM γ-CDx environment. The residual functions are shown below for the respective decays. $^{T}(\lambda_{ex} = 375$ nm, $\lambda_{em} = 550$ nm), ^{N} ($\lambda_{ex} = 375$ nm, $\lambda_{em} = 450$ nm).

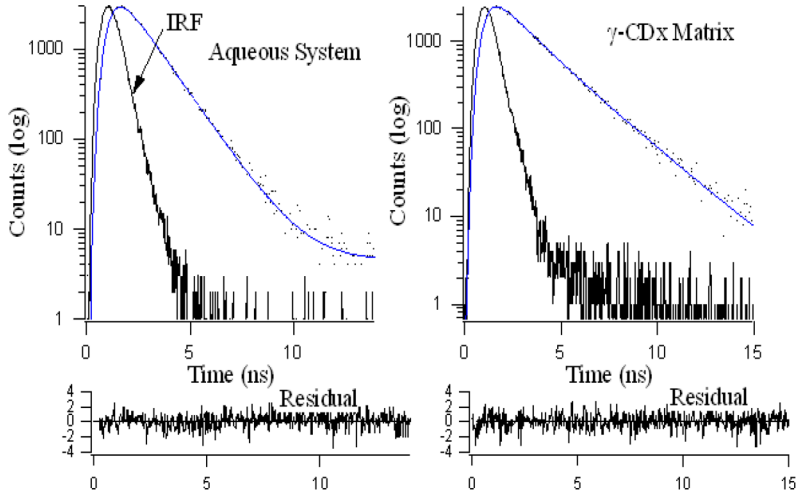

Figure 4.

Single and bi-exponential fluorescence decay profiles for 10 μM daidzein in aqueous and 20 mM γ-CDx environments respectively. Residuals are shown below for the respective decays. λ_{ex} = 340 nm, λ_{em} = 470 nm.

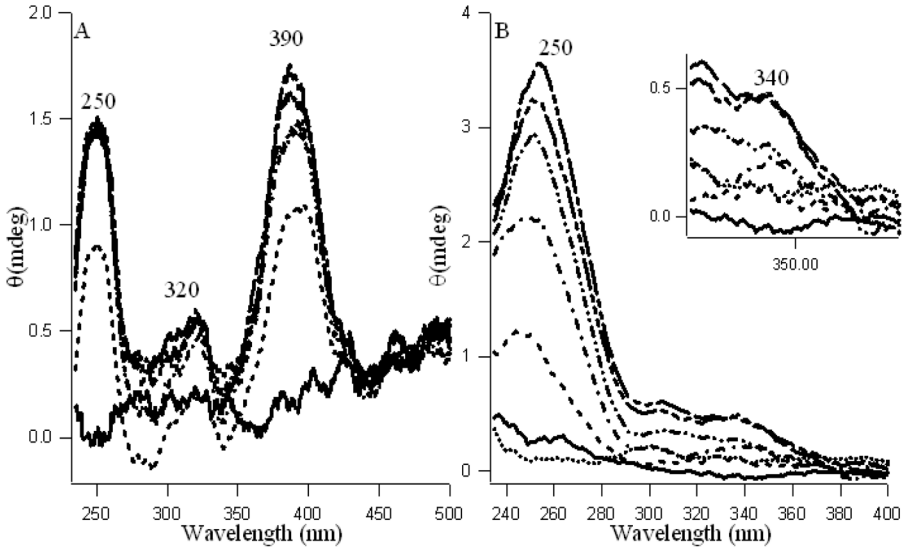

Figure 5.

Induced Circular Dichroism spectra of fisetin (20 μM, A) and daidzein (25 μM, B) with increasing concentration of γ-cyclodextrin (0—, 1 ---, 5 –·–, 10 –··–, 15 –···–, 20 – – --mM). B inset highlights the wavelength 300–400 region of figure B. The dotted line in B shows free γ-CDx.

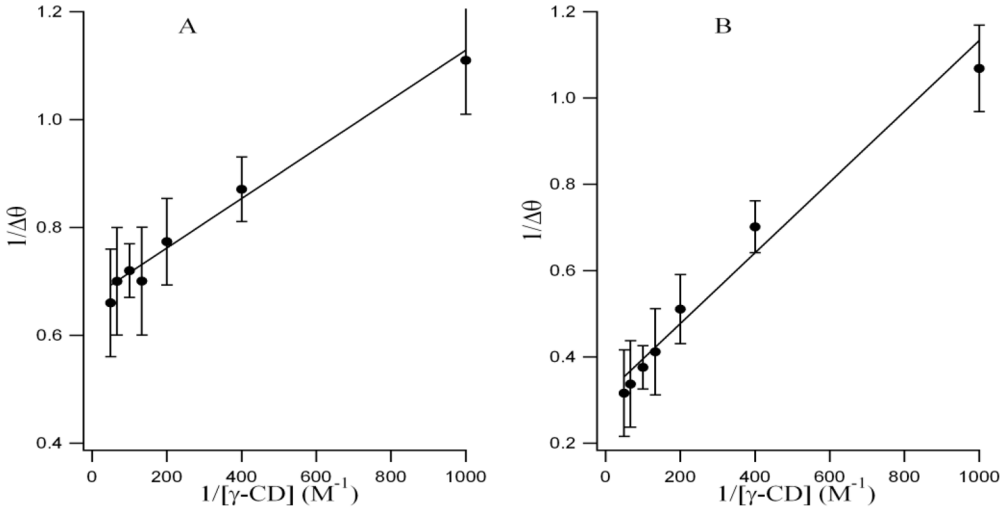

Figure 6.
Double-reciprocal plots (best fit) using induced circular dichroism data for encapsulation of fisetin (A) and daidzein (B) in γ-cyclodextrin.

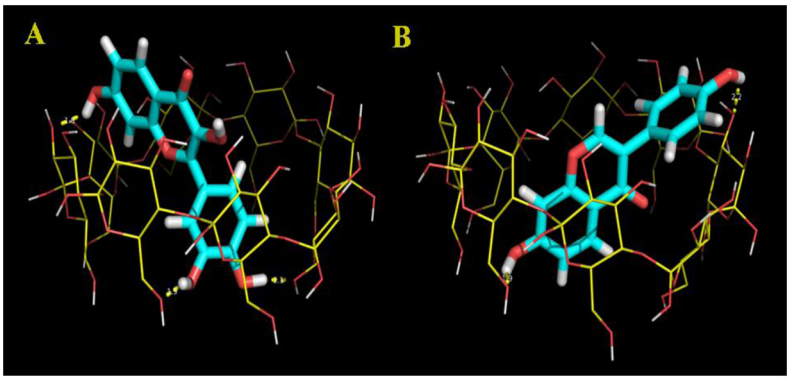

Fig 7.
Lowest energy docked complex of fisetin (A) and daidzein (B) with γ-CDx cavity. γ-CDx is rendered in line representation while the flavonoids are rendered in stick representation.

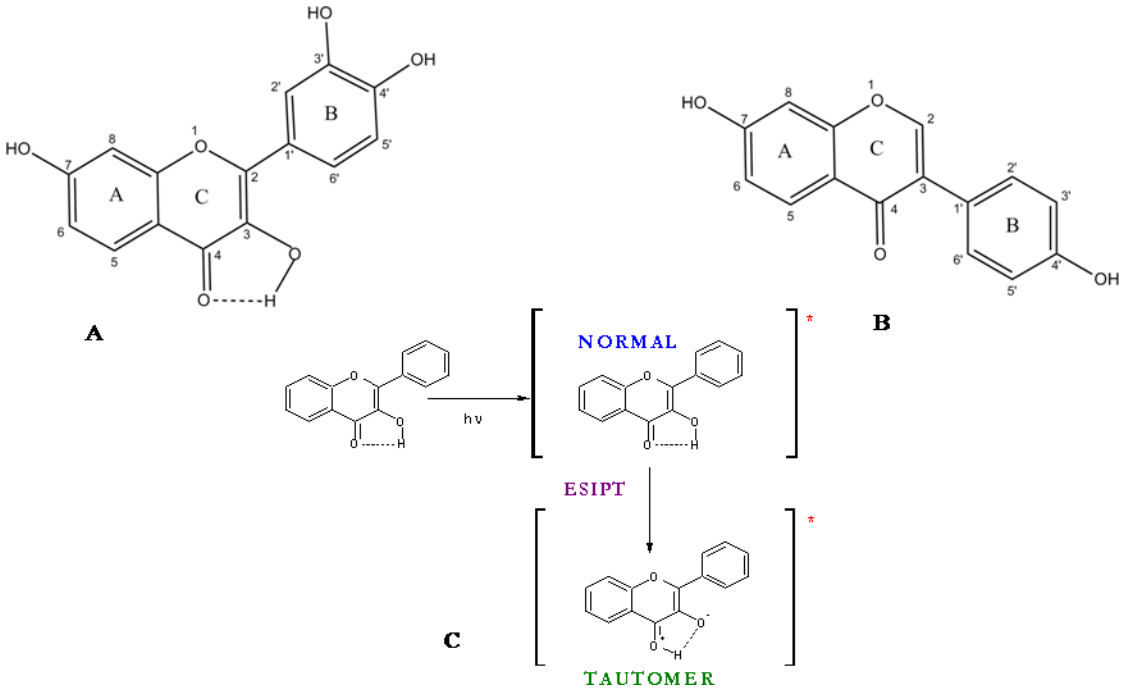

Scheme 1.

Structures of A. Fisetin, B: Daidzein molecules. C: Ground and excited (denoted by *) states of normal (N) and tautomer (T) forms of a flavonol.

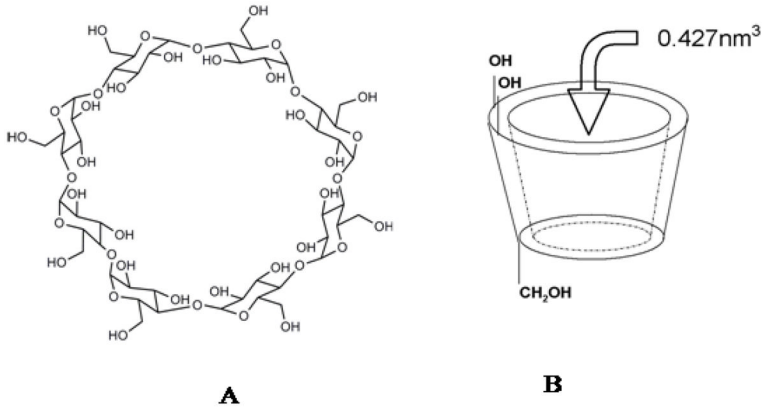

Scheme 2.
Structures of A: γ-cyclodextrin and B: 3D representation of γ-cyclodextrin.

Table 1

Steady state fluorescence emission parameters for fisetin and daidzein in aqueous and γ-CDx environments.

System	Flavonoids	λ_{em}^{max} (nm) (nm) Normal[ab]	λ_{em}^{max} (nm) (nm) Tautomer[a]	Fluorescence Intensity[b] (I_T/I_N) [a]	Anisotropy (*r*)
	Fisetin[a]				
Aqueous system		488	517	1.09	0.03
γ-CD matrix (15 mM)		484	532	1.69	0.114
	Daidzein[b]				
Aqueous system		469		10.67	0.025
γ-CD matrix (15 mM)		467		43.21	0.11

[a] (I_{T530}/I_{N470}),

[b] Fluorescence Intensity at λ_{em}^{max}

For anisotropy measurements: [a] λ_{ex} = 370 nm, λ_{em} = 580 nm, [b] λ_{ex} = 340 nm, λ_{em} = 470 nm

Table 2

Fluorescence decay parameters of fisetin tautomer (Fis (T))[a] and fisetin normal (Fis (N))[b] species in water and in presence of γ-CDx

Sample	τ_1(ns)	τ_2(ns)	τ_3 (ns)	a_1	a_2	a_3	$\bar{\tau}$(ns)	χ^2_r	DW
Fis (T) [a] in water	0.044	1.11	----	0.937	0.063	----	0.715	1.19	1.76
Fis (T)[a] in 10mM γ-CDx	0.18	1.36	6.68	0.551	0.283	0.166	4.99	1.09	1.80
Fis (T)[a] in 20mM γ-CDx	0.17	1.59	6.81	0.453	0.288	0.259	5.55	1.13	1.82
Fis (N)[b] in water	0.011	0.73	----	0.998	0.002	----	0.096	1.16	1.85
Fis (N)[b] in 10mM γ-CDx	0.018	0.75	2.56	0.994	0.005	0.001	0.40	1.18	1.70
Fis (N)[b] in 20mM γ-CDx	0.018	0.63	2.12	0.993	0.006	0.001	0.30	1.11	1.78

γ-CDx solutions are prepared in water, [Fis]= 7.5 μM,

[a](λ_{ex} = 375 nm, λ_{em} = 550 nm),

[b](λ_{ex} = 375 = 450 nm), FWHM ≈ 115 ps,

$$\bar{\tau} = \frac{\sum_i a_i \tau_i^2}{\sum_i a_i \tau_i}$$

Table 3

Fluorescence decay parameters of Daidzein in aqueous system and γ-CDx matrix

Sample	τ_1 (ns)	τ_2 (ns)	τ_3 (ns)	a_1	a_2	a_3	$\bar{\tau}$ (ns)	χ^2_r	DW
Daid in water	1.32	----	----	1.0	----	----	1.32	1.04	1.84
Daid + 10mM γ-CDx	1.50	2.55	----	0.68	0.32	----	1.97	0.99	1.86
Daid+ 20mM γ-CDx	1.32	2.38	----	0.41	0.59	----	2.09	1.07	1.79

$$\bar{\tau} = \frac{\sum_i a_i \tau_i^2}{\sum_i a_i \tau_i}$$

(λ_{ex} = 340 nm, λ_{em} = 470 nm), FWHM ≈ 935 ps,

γ-CDx solutions are prepared in water, [Daidzein] = 10 μM